A NOMOGRAPHIC METHOD FOR EVALUATING X-RAY BACK-REFLECTION PATTERNS USED IN THE COMPUTATION OF RESIDUAL STRESSES IN STEELS

By

I. S. Szántó

Department for Mechanical Technology of the Polytechnical University, Budapest

(Received March 25, 1957)

1. Introduction. Scope of the present paper

Measurements of stresses, resp. lattice strains in metals by X-ray diffraction patterns are usually performed by using the back-reflection arrangement. There are two methods the most frequently used for evaluating the patterns thus determined, the so-called reflectograms [1]:

a) by determining the shift of diffraction line peaks, caused by an appropriately indicating array of atomic planes, or

b) by analyzing the profile of the interference lines concerned.

Application of both methods appears to be most favourable, if permitted by test conditions, first of all by metallographic conditions of the specimen investigated. Criteria for the latter, as well as the computation of a new parameter of state rationally indicating the material's intrinsic properties — e. g. internal stresses — to be obtained from complex evaluation are dealt with by the author elsewhere [2].

However, for production routine measurements of an informative character, a rapid and not too complicated method had to be developed, so as to provide for an easier evaluation of reflectograms, ensuring the relative minimum for possible errors. The idea to select a graphic method, for this purpose, seems to be obviously sound. Plotting recorded data into nomograms appears to be a most desirable type of solution.

The scope of the present paper is to try developing a method for the graphic evaluation of X-ray back-reflection patterns, ensuring an accuracy generally satisfactory for common requirements, being still simple enough to dispense with the employment of qualified labour in order to perform actual measurements.

2. Outlines of the applied X-ray technique

Lattice distortions or strains caused by residual or locked-up stresses can be directly measured by X-ray diffraction patterns. In this respect the X-ray technique is similar to other known methods of stress measurement based mostly

on tensometric principles. The latter methods record the relative elongation or strain along a gauge length of macroscopic dimensions, the former method employs one of the magnitude of several Ångström units to definite strain. Stress variations with steep slopes of a local character may be observed, too. The high sensitivity of this procedure, on the other hand, is a potential backdraw, because it introduces several new error sources. Thus a fault caused by less precise evaluation of the X-ray diffraction patterns will trend more easily to erroneous results, than any other macroscopic method of less sensitivity. A graphic method of evaluation, that practically excluds the errors in the order of magnitude, is therefore highly desirable.

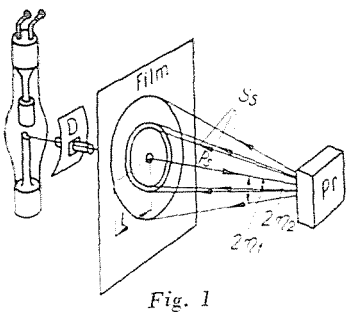

Fig. 1

A detailed analysis of all experimental conditions would exceed the scope of the present paper. The basic principles of the applied method are supposed to be known. A schematical arrangement of the back-reflection X-ray technique is discussed here — as shown in Fig. 1 — only as far as it constitutes the fundamental basis for the proposed method of evaluation.

Around the primary beam P_s of X-rays limited and collimated by the diaphragm D, as around an axis, a full set of separate cones formed by the secondary rays S_S reflected from the specimen P_r is obtained. Intersections of these cones with the recording planes of the surface result in the characteristic Debye-rings seen on reflectograms. These rings are circular only in the case of normal incidence ; in the common case of oblique incidence they are deformed into quasi-ellipses. The half-diameter of the ring (i. e. in fact is an interference line) is denoted by l. These latter values measured on diffraction photographs are taken as the initial data for the evaluation.

Within the specimen, the stress σ to be measured and causing strain, is acting in a plane perpendicular to P_s or parallel to it. In case of tensile loads (Fig. 2) some contraction of the crystallites — shown symbolically, as of polygonal shape — is obtained in the direction of the primary beam of the X-rays. So far as the microstructure is concerned, this process may be taken as a reduction in the interatomic distances between atoms lying in the same direction. In reality, no contraction in the direction of P_s, but only distances $d_{\perp}$ between atomic

planes in direction of the normal N of the set of planes can be measured, because actually the array of atomic planes defined by the normal N can only produce reflections. This normal N includes an angle η with the direction of the incident beam of X-rays, while reflection is defined by the angle 2η. The reduction Δd of the distance $d_\perp$ as caused by the stress σ will be, therefore, a projection in the direction of N of the true compression strain (contraction).

3. Fundamentals of interpretation

Generalized for an arbitrary direction of measurement X: If the lattice parameter of an unstressed specimen is d_0, while the same for the stressed one

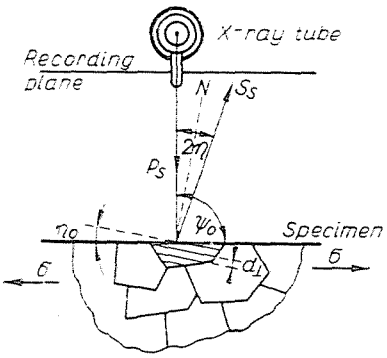

Fig. 2

is d_x, correspondingly the half-diameter of an interference ring on the reflectogram taken from the unstressed specimen is l_0, while l_1 to be measured on a reflectogram obtained from a stressed specimen, then for known distance T_a between the surface of the specimen and the recording plane the complementary reflection angle η and by using the latter the lattice parameter d may be determined by using the following relations :

$$\eta_0 = \frac{1}{2} \cdot \operatorname{arc\,tan} \frac{l_0}{T_a} \qquad (1/a)$$

$$\eta_x = \frac{1}{2} \cdot \operatorname{arc\,tan} \frac{l_x}{T_a} \qquad (1/b)$$

$$d_0 = \frac{\lambda}{2 \cos \eta_0} \qquad (2/a)$$

$$d_x = \frac{\lambda}{2 \cos \eta_x} \qquad (2/b)$$

where λ is the wavelength of the monochromatic X-ray beam used for the investigation.

The unit strain (contraction) in direction X characterizing the lattice deformation is defined by

$$\varepsilon_x = \frac{d_x - d_0}{d_0} = \frac{\triangle d}{d_0} \tag{3}$$

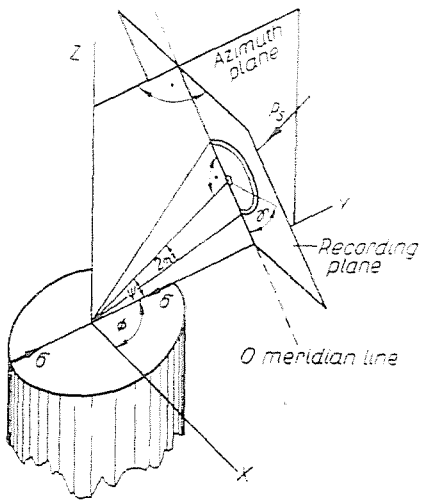

Fig. 3

The accuracy of the determination of the value of ε_x by X-ray measurements will, therefore, depend upon the fact, whether we succeed in choosing a test arrangement, i. e. relative spatial position of the specimen and the recording film cassette so as to be able to deduce from the reflectograms values d_{hkl}, indicating most sensitively all lattice changes. Geometric conditions for the back-reflection arrangement are definitely given by the following angles shown on Fig. 3 :

a) η ... complementary reflection angle (complementary angle of the Bragg angle Θ);

b) ψ ... angle included by the primary X-ray beam and the specimen surface;

c) γ ... angle defining the direction of the Debye- ring radius with reference to the zero-meridian line;

d) Φ... angle defining the direction of the principal stress acting in the plane of specimen surface and the azimuth plane of the arrangement.

By using the above characteristics, we can compute for each case the so-called *sensitivity factor* (S), by use of which the value of ε_x measured by diffractometry in the direction of X, can be reduced to ε_1, i. e. the unit strain in the direction of the principal stress, directly influenced by the σ_1 to be determined. On the other hand we have, also, numerical information about the sensitivity of recording, on the measurement in the direction of X. Maximum sensitivity is obtained for the case $S = 1$, while total unsensitivity is reached by certain preferred orientation ψ^*, resulting in $S = 0$. The introduction and computation of the factor S is being dealt with elsewhere [2]. Without recurring to deductions, we only mention here that in case of uniaxial stress state ($\Phi = 90°$), as well as for any angle ψ of irradiation and for given angles η and γ the sensitivity factor is obtained by numerical substitution into the following expression :

$$S_x = \frac{\varepsilon_x}{\varepsilon_1} = \cos^2\eta \cdot (\cos^2\psi - \nu \cdot \sin^2\psi) + \sin^2\eta\,(\sin^2\psi - \nu \cdot \cos^2\psi) \cdot \cos^2\gamma - \\ - \nu \cdot \sin^2\eta \cdot \sin^2\gamma + \frac{1+\nu}{2} \cdot \sin 2\psi \cdot \sin 2\eta \cdot \cos\gamma \qquad (4)$$

where ν denotes Poisson's ratio, which may be taken as a constant for steels.

The conditional equation for total insensitivity (strain invariancy) of measurement is given in our case by

$$\tan^2(\psi^* + \eta) = \frac{1}{\nu} - \frac{\cos^2\Phi}{k} \qquad (5)$$

where

$$k = \frac{\nu}{1+\nu} \qquad (6)$$

We may assume a value of $\nu = 0{,}3$ for ferrous alloys. In performing the test at a setting of $\Phi = 90°$, the preferred angular orientation of the invariant direction of measurement (ψ^*) may be summarized in Table I for the usual X-ray radiations.

Table I

Incidence angles (ψ^*) for the usual X-ray radiations

Radiation	Indices (*hkl*) of indicating set of atomic planes	Direction of N normal	Preferred incidence angle value resulting in invariant half-diameter for $\gamma = 180°$
Co—K_{α_1}	(310)	9° 19′ 30″	51° 58′ ≈ 52°
Cr—K_{α_1}	(211)	11° 57′ 20″	49° 20′ 10″ ≈ 49°
Fe—K_β	(310)	14° 19′ 02″	46° 58′ 28″ ≈ 47°

A setting error of less than 1° during exposure preparations would not influence the measurement result more, than, if the value of ν would be assumed as 0,28, which is still acceptable for strength calculations.

The computation of the invariant directions as shown in the above simplified case will gain special importance in duplex X-ray technique, where it will be allowed to determine reference data for the unstressed state from a loaded specimen [3]. This technique will be described in detail, in a later paper.

Numerical values of the sensitivity factors S for the usual perpendicular and 45° oblique primary beam incidences, as well as for the invariant angular positions already mentioned are summarized in Table II, using relation (4) for computations.

Table II

Sensitivity factors as a function of angular setting.
(Basic particulars to the Diagram IV).

ψ	S_x	Co—K_{α_1} radiation		Cr—K_{α_1} radiation		Fe—K_β radiation	
		$\gamma = 0°$	$\gamma = 180°$	$\gamma = 0°$	$\gamma = 180°$	$\gamma = 0°$	$\gamma = 180°$
45°	$S_{+/45}$	0,558		0,613		0,661	
	$S_{-/45}$		0,143		0,086		0,039
47°	$S_{+/47}$					0,622	
	$S_{-/47}$						0
49°	$S_{+/49}$			0,521			
	$S_{-/49}$				0		
52°	$S_{+/52}$	0,403					
	$S_{-/52}$		0				
90°	$S_\perp$	—0,266		—0,244		—0,221	

A correct evaluating procedure necessitates introduction of a logical convention so far as notation technique is being concerned. It can be performed by substituting the value of incidence angle ψ in place of the generally used index x for both ε and S values, as well as by a reference to the fact, whether evaluation is based on the part of the Debye-ring adjacent to the specimen, where $\gamma = 0°$ and the index e. g. $_{+/45}$, or on a half-diameter for the far side ($\gamma = 180°$ and the index e. g. $_{-/45}$). The two dimensions l can become equal only for $\psi = 90°$ i. e. for perpendicular direction of incidence, denoted by an index: $_\perp$. It should be noted that in this case the sum of the two principal stresses, parallel to the surface of the object, that is σ_1 and σ_2, can be measured.

4. Graphic procedure

Using the principal scheme already described, different steps of the graphic evaluation procedure is summarized in the following paragraphs :

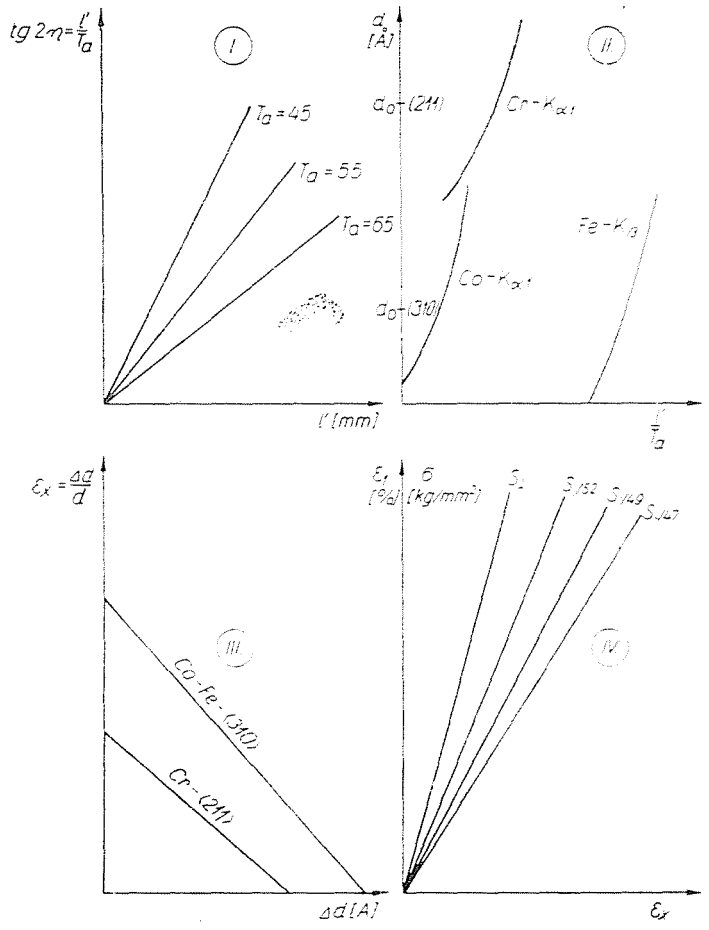

Fig. 4

1. After adjusting the value l read from the reflectogram according to the corrections seemed necessary and also known from the literature [4] (taking into account film shrinkage, shift due to oblique incidence, etc.) the corrected half-diameter l_k is computed.

2. The distance T_x between specimen surface and recording plane is determined, either by an indirect method using a reference material, or by a direct one using the internal screw gauge, and a combined film camera, etc.

3. After choosing the parameter T_a found in Diagram I (Fig. 4) and as approximate to T_x as closely as possible, the value of l_k is modified by multiplying through the ratio $\frac{T_x}{T_a}$ to obtain l'.

4. Using Diagram I we find the value of $\tan 2\eta = \frac{l'}{T_a}$ corresponding to the value of l' already obtained.

5. Choose on Diagram II the curve corresponding to the primary X-ray radiation used (e. g. that for the Co—K_{α_1}), whereafter we project the already known ratio $\frac{l'}{T_a}$ to obtain the value of the lattice parameter d corresponding to l.

6. Plot the section between the ordinate points d and d_0 and transfer it to the horizontal scale Δd of Diagram III.

7. Draw a parallel to the corresponding directrix of Diagram III from the end point of the section Δd, by the position of which on the scale of ordinates $\left(\text{having a dimension of } \frac{\Delta d}{d}\right)$ will be located in a distance giving the value of ε_x to be determined.

8. Starting from ε_x on Diagram IV and choosing from the set of lines S the line S_x characteristic of the test arrangement, we may determine the value of the unit strain ε_1 through perpendicular projection. As this differs from the corresponding value σ_1 only by a constant coefficient (i. e. Young's modulus : E), by use of a suitably chosen scale, we may directly read off the magnitude of the stress σ_1 acting in direction Φ in the adjacent range of the specimen surface and causing a unit strain ε_1.

The use of Diagram II seems to be the most critical process. The reason for this is, because the coordinates $\frac{l'}{T_a}$ resp. d will fall into different numerical ranges according to the X-ray radiation (Table III). It is therefore advisable to construct separate diagrams for each sort of X-rays, which also give us the possibility to choose a suitably large scale, whereby unreliable and inaccurate oblique line crossings should be avoided. Under these circumstances it appears obvious to unite Diagrams I and II according to that shown on Diagram V (Fig. 5). Similarly one finds it advisable to contract Diagrams III and IV into a single graph. This has been done in Diagram VI. The general procedure of graphic evaluation is shown by a concrete numerical example. Subsequent steps of construction as given by the dotted lines, the direction being shown by the arrows and the order of succession by the numbers according to the lines. Sequence numbers 4 to 8 are identical with those of operational phases enumerated during the short description of graphic procedure.

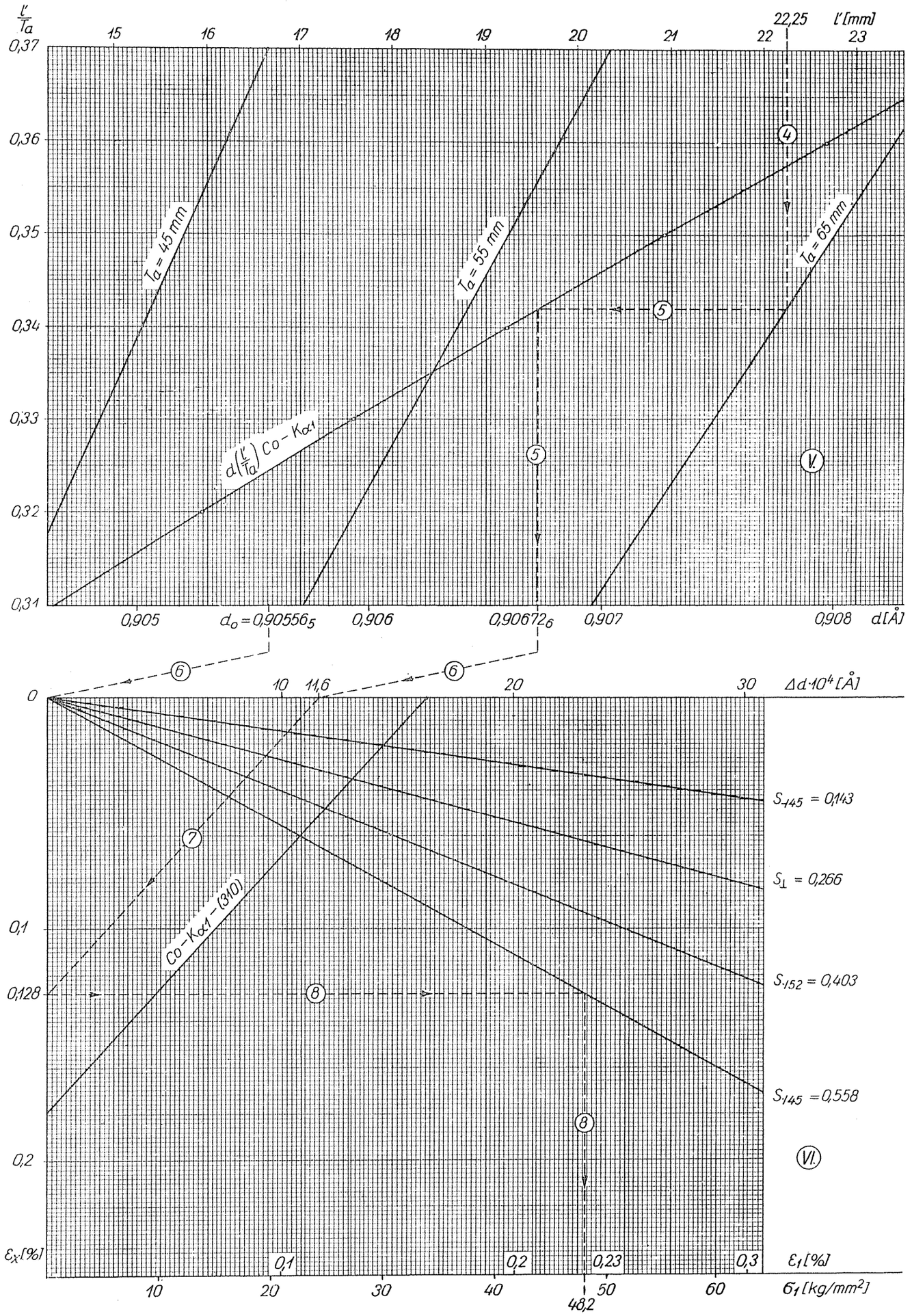
l'/Ta
15
16
17
18
19
20
21
22
22,25
l'[mm]
23
0,37
0,36
0,35
0,34
0,33
0,32
0,31
Ta = 45 mm
Ta = 55 mm
Ta = 65 mm
d(l'/Ta) Co - Kα1
4
5
5
V.
0,905
d₀ = 0,905565
0,906
0,906726
0,907
0,908
d[Å]
6
6
0
10
11,6
20
30
Δd·10⁴[Å]
7
Co - Kα1 - (310)
8
8
S145 = 0,143
S⊥ = 0,266
S152 = 0,403
S145 = 0,558
VI.
0,1
0,128
0,2
εx[%]
0,1
0,2
0,23
0,3
ε1[%]
10
20
30
40
48,2
50
60
σ1[kg/mm²]

Fig. 5

The magnitude of the resulting section on Diagram V will not only depend on the read d value, but also on the value of d_0 which characterizes the initial state of the steel investigated, and is variable with chemical constitution. The basic value d_0 has the dimension of Ångström units and any possible variation may occur only in the third, or rather the fourth decimal figure. This change will cause no trouble in computing the value of $\varepsilon_x = \frac{\Delta d}{d_0}$, as the value of a quotient is practically uninfluenced by a variation of similar order of magnitude in the denominator. As the slope of the directrix figuring in operation 7 may be assumed as practically constant, if a given reflecting array of atomic planes has been selected for indicating purposes.

However, the variation of d_0 will significantly influence the value of the difference $\Delta d = d - d_0$. As the first three decimals of both diminuend and subtrahend are usually identical, significant figures of Δd are delivered by the fourth, fifth and (mostly by appraisal) by the sixth decimal figures. Any variation in d_0 will therefore play an important role when computing the value of Δd. The result of this will be during the graphical procedure, that d_0 will change its locus on Diagram V. This must be repeatedly defined for each new kind of steel, however, for X-ray photograph series taken from the same specimen, it will remain constant. After choosing the value of d_0 it would be advisable to move Diagram VI parallel to itself (to the right in our example), so that the origo of the upper Δd scale will fall under point d_0 of Diagram V. In this case the resulting intersection on Diagram V may be used directly — without recurring to the projection 6 — for the subsequent phase 7 of the evaluating procedure. By preparing Diagram VI on a transparent sheet, thus rendering it suitable to be used on both sides, not only the increment upward from d_0 (elongation), but also the decrement taken downward from it (contraction) may be directly projected after reversing the diagram.

It should be noted that the nomograms which are reproduced are reduced to scale for typographical reasons. Actual graphs used by us for successful graphic evaluation procedure had been prepared in size 59 by 40 cms, so that Diagrams V and VI are here reduced. The problem of suitable scale choice is dealt with in the following chapter in connection with accuracy control of graphic evaluation.

5. Discussion

Determination of residual stresses — so far as X-ray technique is concerned — is equivalent to precision measurement of lattice parameters. The character of error sources and possibilities of correction during accurate measurements of lattice dimensions have already been dealt with in detail elsewhere [5]. In the present paper we want mainly to investigate the factors which especially in-

fluence graphic evaluation procedure; features of the evaluating operation limiting accuracy of measurement will be discussed forthwith.

It is generally known that evaluation is most intensively affected by

1. physical (metallographic) properties of the material investigated (η, d_0)

2. geometric circumstances determining the testing arrangement (ψ, Φ, γ, T_a)

3. objective error sources due to recording (systematic errors) and

4. subjective uncertainty factors of reading (δl, δT).

ad 1. The values of the angle η and d_0 will become — in first approximation — constant quantities, after the selection of the primary X-ray radiation. As will be shown below, the value of the complementary reflection angle is a most decisive factor for the sensitivity of measurement.

ad 2. The effect of setting angles is included during the course of evaluation in the sensitivity factor S. Its numerical value is an absolute parameter of measurement sensitivity. We will also return later to discuss the influence of the distance T_a.

ad 3. Systematic errors of recording apparatus (film, G-M-counter, comparator, microphotometer) can be always corrected by careful control tests. Their influence may be omitted when analyzing the accuracy of the procedure.

ad 4. Among subjective reading errors, inaccuracies in the measurement of distances l and T will dominate. The errors of measurement δl and δT will be inherited by subsequent operations of the evaluation procedure, or it may even increase, if the value of δl will accumulate additional secondary uncertainty factors in the course of graphic procedure. So as the following which is more detailed.

The precision of the final result of operations will be characterized by the relative value $\frac{\Delta d}{d}$ while error limits will be given by the quantity $\pm \Delta d$. The procedure of error analysis will, generally, start by computing the differentials of the functions used, as the basis of evaluation, and expressing it by the partial derivatives of all quantities figuring in the functions [6]. By assuming these differentials as error limits, we may compute the accumulated error at the end of graphic evaluation.

As is well-known, the functions (1) and (2) forming the basis of evaluation are continuous and can be differentiated. Thus the differential can be formed according to the formula:

$$\delta d = \frac{\partial d}{\partial T} \cdot \delta T + \frac{\partial d}{\partial l} \cdot \delta l \tag{7}$$

Table III

Groups of characteristic data for accurate plotting of Diagram II

radiation									
Co—K_{α_1}	$\frac{l'}{T_a}$	0,31	0,32	0,33	0,34	0,35	0,36	0,37	0,38
	η_{grad}	8°36′42″	8°52′20″	9°07′53″	9°23′20″	9°38′42″	9°53′58″	10°09′08″	10°24′12″
	d Å	0,904649	0,905282	0,905931	0,906595	0,907274	0,907969	0,908677	0,909400
Cr—K_{α_1}	$\frac{l'}{T_a}$	0,36	0,37	0,38	0,39	0,40	0,41	0,42	0,43
	η_{grad}	9°53′58″	10°09′08″	10°24′12″	10°39′10″	10°54′02″	11°8′48″	11°23′28″	11°38′02″
	d Å	$1{,}16212_0$	$1{,}16303_0$	$1{,}16395_5$	$1{,}16488_6$	$1{,}16585_6$	$1{,}16683_0$	$1{,}16782_4$	$1{,}16883_3$
Fe—K_β	$\frac{l'}{T_a}$	0,51	0,52	0,53	0,54	0,55	0,56	0,57	0,58
	η_{grad}	13°30′39″	13°44′13″	13°57′42″	14°11′04″	14°24′19″	14°37′28″	14°50′30″	15°03′30″
	d Å	0,903374	0,904139	0,905023	0,905896	0,906786	0,907682	0,908590	0,909508

The latter may be transformed into

$$\frac{\delta d}{d} = \frac{1}{d} \cdot \frac{\partial d}{\partial T} \cdot \delta T + \frac{1}{d} \cdot \frac{\partial d}{\partial l} \cdot \delta l \tag{8}$$

After re-arranging function (1) and determining its partial derivative (for $T =$ $=$ const) we obtain

$$\delta l = \frac{2T}{\cos^2 2\eta} \cdot \delta\eta \tag{9}$$

Differentiating function (2) against variable d results in

$$\frac{\delta d}{d} = \tan\eta \cdot \delta\eta \tag{10}$$

By substituting equation (9) into expression (10) we arrive at

$$\frac{\delta d}{d} = \frac{1}{2} \cdot \tan\eta \cdot \cos^2 2\eta \cdot \frac{\delta l}{T} \tag{11}$$

By determining the partial derivative of function (1) for $l =$ const we have

$$\delta l = \delta T \cdot \tan 2\eta + \frac{2T}{\cos^2 2\eta} \cdot \delta\eta = 0 \tag{12}$$

Substituting $\delta\eta$ again from (10), we may write after re-arranging and simplifications :

$$\frac{\delta d}{d} = -\frac{1}{4} \cdot \frac{\delta T}{T} \cdot \sin 4\eta \cdot \tan\eta \tag{13}$$

In order to estimate the summarized error of the measurement of d the following term may be obtained by summation of the absolute values of (11) and (13):

$$\left|\frac{\delta d}{d}\right| = \underbrace{\left|\frac{1}{4} \cdot \tan\eta \cdot \sin 4\eta\right|}_{A} \cdot \left|\frac{\delta T}{T}\right| + \underbrace{\left|\frac{1}{2} \tan\eta \cdot \cos^2 2\eta\right|}_{B} \cdot \left|\frac{\delta l}{T}\right| \tag{14}$$

It should be noted that with decreasing angle η the error will increase somewhat because of the expression $\cos^2 2\eta$, while on the other hand $\tan\eta$ and $\sin 4\eta$ will intensively reduce the total error (see Table IV).

Table IV

The influence of the reflection angle on the precision of measurement

Radiation	$\tan \eta$	$\sin 4\eta$	$\cos^2 2\eta$	A	B	$A\frac{\delta T}{T}\cdot 10^5$	$B\frac{\delta l}{T}\cdot 10^5$
Co—Kα_1	0,1644	0,6065	0,897	0,0250	0,0737	2,5	2,9
Cr—Kα_1	0,2126	0,7431	0,834	0,0394	0,0886	3,9	3,6
Fe—Kβ	0,2555	0,8418	0,769	0,0536	0,0980	5,4	3,9

Note: Values shown in the last two columns are valid for $\frac{\delta T}{T}=0{,}001$ and $\frac{\delta l}{T}=0{,}0004$.

It follows from relation (14) that under identical exposure conditions the resulting error will become less

a) the greater the distance T

b) the smaller the angle η

c) the smaller the inaccuracy δT of measurement

d) the smaller the reading uncertainty δl.

ad a) Any increase in the value of T may be regarded rational only up to a certain limit. The distance between the specimen and the recording film holder does not usually exceed 60—70 mms. Above this limit the time of exposure will increase, so as to render the tests uneconomical; on the other hand the lines themselves will also gradually broaden. Any increase in measuring accuracy by this method (see Table V) can be only of theoretical interest taking in view the ever increasing disadvantages.

ad b) The value of the complementary reflection angle η may be varied by discrete quantities. Its lowest value is obtained by using the Co-K$_{\alpha 1}$

Table V

A comparison of measurement error limits for different exposure conditions and line profiles of medium sharpness

Radiation	T_a	δT	δl	$\frac{\Delta d}{d}10^5$	$\pm \Delta d\cdot 10^5$ error Å	Measurement error in direction					
	mm					· /45	· /47	· /49	· /52	⊥	—/45
						$\pm \Delta\sigma$ kg per sq. mm					
Co—K$_{\alpha 1}$	50	0,05	0,02	5,4	4,9	2,0			2,8	4,3	8,0
Cr—K$_{\alpha 1}$				7,5	8,8	2,6		3,0		6,4	18
Fe—K$_\beta$				9,3	8,4	2,9	3,1			8,8	∞
Co—K$_{\alpha 1}$	65	0,05	0,02	4,2	3,8	1.6			2,2	3,3	6,2

radiation, while its maximum is attained by the Fe-K_β radiation. Dependent on metallographic reasons we are quite often forced to use also the radiation Cr-K_{α_1} characterized by medium η angle values [7]. The final error limit of measurement is greatly influenced by the factor S characteristic of the geometric arrangement. As seen from Table II, in the case of oblique primary-beam incidence S will indicate the most favourable effect for the Fe-radiation, while having the least influence on the Co-K_α radiation. Because of the opposing effects the error of measurement $\pm \triangle\sigma$ will be — contradictory to common belief — largely compensated, as indicated by Table V.

ad c) Any reduction of the error δT is a problem of measurement technique. Graphic evaluation will not magnify this error, although it will not reduce it. Even under the most unfavourable conditions of distance measurements it can be quite easily attained that the error of accurate T determination shall not exceed 0,05 mm.

ad d) Uncertainty factor δl caused by reading can be generally reduced to $\pm$ 0,02 mm in case of line profiles of medium sharpness (taken on a ring diameter of 2 l). This accuracy limit appears as a zone of uncertainty in the diagrams. By taking the most difficult handling of scale of Diagram VI, i. e. that of $\triangle d$ (this scale has been chosen as 1 mm equals 2.10^{-5} Ångström units), we find that the error range resulting from δl has a width of about 2,5 mm, in this phase of the evaluation. The accuracy of graphic construction will in every case exceed this value. Thus, during the graphic evaluation procedure, even if the error of the result is increasing, the deviation will remain within the zone resulting from the subjective determination of the position of the line peaks. Similarly, no difficulties have been encountered during graphic evaluation (using the diagram scales as already given) because of the finite thickness of pencil trace.

However, on the actual nomograms, the scales had to be increased. The reason for this that on Diagram V the desired measurement accuracy could only be obtained, if the scale of l' had been already magnified by 2,5. So it became possible to plot measured ring half-diameters within an accuracy limit of 0,02 mm on the axis of abscissae. (True scale : 1 mm on the diagram equals 0,02 mm on the film.) In order to transfer intersecting distances directly, Diagram VI has also been enlarged in the same scale as Diagram V. Any further enlargement of the scale would only give a fictive increase on the reliability of construction. As a consequence, the large size nomograms could not be easily handled, and besides the resulting accuracy would not increase. The error is defined, namely, by the measured quantity having the highest uncertainty factor (i. e. l). Thus, other quantities which could be defined with a higher accuracy are not worthy of being elaborated more precisely.